
CNT and proteins for bioelectronics in personalized medicine

Andrea Cavallini, Cristina Boero, Giovanni De Micheli and Sandro Carrara

From their discovery, CNTs have increasingly attracted interest because of their peculiar electrical, mechanical, and chemical properties. In 1991, Sumio Iijima first observed and described in detail the atomic arrangement of this new type of carbon structure [1]. By a technique used for fullerene synthesis, he produced needle-like tubes at the cathode of an arc-discharge evaporator. From that time, carbon nanotubes have been used for many applications and represent one of the most typical building blocks used in nanotechnology. Their peculiarities include unique properties of field emission and electronic transport, higher mechanical strength with respect to other materials, and interesting chemical features.

The use of CNTs has recently gained momentum in the development of electrochemical biosensors, since their utilization can create devices with enhanced sensitivity and detection limit capable of detecting compounds in concentrations comparable to those present in the human body.

This chapter will review the most important features of carbon nanotubes, and present an example in which their application can enhance the detection of drugs and metabolites relevant in personalized medicine: P450 biosensors for therapeutic drug monitoring.

9.1 Overview

Carbon is a very interesting element, since it can assume several stable molecular structures. Any molecule entirely composed of carbon is called a fullerene. It can assume the

form of hollow spheres, needles or ellipsoids [2]. Graphene is an allotrope of carbon, where atoms are arranged in sp^2 bonding state, with hexagonal honeycomb lattices arranged in a seamless structure. Graphene sheets can be stacked one on the top of the other to form graphite, the most popular form of carbon structure. Single or multiple graphene sheets can also be rolled along a lattice vector of the sheet and form a carbon nanotube. Depending on the number of rolled sheets, it is possible to identify two categories of nanotubes: single-walled carbon nanotubes (SWCNTs) and multi-walled carbon nanotubes (MWCNTs). The different chemical structure confers different properties on these types of carbon nanotubes. Single-walled carbon nanotubes consist of a single cylinder with a diameter of 0.4–2 nm. SWCNTs can be metallic or semiconducting (including small-bandgap semiconductors), depending on their chirality and diameter. The chirality refers to the alignment of the π -orbitals when the graphene sheet rolls up [3]. Different configurations of chirality confer different conducting properties. Around two-thirds of SWCNTs are semiconductors and one-third are metallic. Recently, several researches have proposed methods to separate SWCNTs according to their different conducting properties. Krupke *et al.* were able to separate semiconducting from metallic SWCNTs by using alternating current dielectrophoresis [4]. An alternative method proposed by Chattopadhyay *et al.* functionalizes SWCNTs with amines [5]. Amine groups have much more affinity with semiconducting than with metallic SWCNTs, promoting the precipitation of SWCNTs on polar ethers. Coaxial multilayer graphene sheets instead form

MWCNTs. The diameter ranges from 1.4 to 100 nm, depending on the number of rolled layers and hollow diameter, while the interlayer space is 0.34 nm [6]. MWCNTs possess metallic properties, which make them suitable as electrodes.

The tips and the walls have different electrical and physical properties. The walls are highly hydrophobic, which is why the tubes have the tendency to coagulate in aqueous solution. The ends, instead, often terminate with oxygenated species, which confer quite hydrophilic properties. Because of that behavior, carbon nanotubes are often dispersed in non-polar organic solvents; surfactants or water-soluble polymers are used to disperse them in aqueous solutions.

9.2 Synthesis of carbon nanotubes

CNT synthesis essentially requires the pyrolysis¹ of a carbon source, such as hydrocarbons or carbon monoxide. Metal nanoparticles serve both as nucleation sites for the vapor molecules and as catalysts to reduce the activation energy needed for the decomposition of the hydrocarbon vapor [7]. Arc-discharge evaporation was the first method used by Iijima to produce carbon nanotubes in 1991 [1]. Laser ablation and chemical vapor deposition (CVD) are the other two common techniques for carbon nanotube synthesis. Arc-discharge evaporation and laser ablation use solid-state carbon as a precursor for nanotubes. The growing temperature is typically high, around thousands of degrees Celsius. CVD takes place at lower temperatures, generally 500–1000 °C, using metal catalyst particles as growing starters and hydrocarbon gases as carbon suppliers. The first two methods are able to produce high-quality carbon nanotubes with near-perfect structure, since they are well-established techniques. However, none of the described methods allows us to produce CNTs with controlled chirality and homogeneous diameters [8].

CNT synthesis inevitably introduces some impurities, such as metal atoms as defects in the graphite structure, amorphous carbon, and structural defects that can be exploited to confer specific electrochemical properties to the nanotube.

Purification steps are often used for both types of carbon nanotubes. Nitric acid and sulfuric acid are often used to remove nanotube caps and leave open-ended tubes. Such treatments eliminate metallic impurities and create dangling bonds on the tubes, which allow further functionalization with oxygenated groups, such as quinones and carboxylic groups.

¹ Pyrolysis is a thermochemical decomposition of organic material at elevated temperatures in the absence of oxygen (or any halogen). It involves the simultaneous change of chemical composition and physical phase, and is irreversible.

9.3 Structure of CNTs

Carbon structure reactivity is primarily dictated by the pyramidalization angles of the carbon atoms. According to the number of atoms surrounding one carbon atom, it is possible to distinguish different configurations. In the case of graphene and its arrangements, two configurations are possible: sp^2 -hybridized (trigonal) structure and sp^3 -hybridized (tetrahedral) structure. The first configuration is planar (graphene) and it does not require pyramidalization angles, whereas the second implies an angle of 19.5°. Among those two stable configurations, more pyramidalization angles exist, for instance in the case of C_{60} with pyramidalization angles of 11.6°. SWCNTs are 1D cylindrical aromatic macromolecules. Pyramidalization angles and misalignment of the orbitals induce curvature of the surface and a local strain. That is the reason that carbon nanotubes are expected to be more reactive than a flat graphene sheet.

Carbon fullerenes and the sidewalls of carbon nanotubes are both curved, but chemically different. First of all, fullerene is curved in 2D, whereas the nanotubes are curved in 1D. Thus, carbon bonds in fullerene are more distorted than those belonging to nanotubes. Pyramidalization angles for carbon atoms of a nanotube can be about 3.0°, while the angle of a fullerene with equivalent radius is 9.7°. The strain energy of pyramidalization is almost proportional to the pyramidalization angle, so fullerene should support about 10 times the strain energy of pyramidalization per carbon atom than an equivalent carbon nanotube of the same diameter.

Carbon nanotubes can be broken down into end caps and sidewalls. The end caps resemble a hemispherical fullerene, and their curvature is higher than the sidewall curvature. Since it is not possible to reduce the pyramidalization angles of any fullerene below 9.7°, this ensures that end caps will always be more reactive than the sidewalls, regardless of the nanotube diameter. Although all the carbon atoms are equivalent, there are two types of bonds: those that run parallel to the circumference and those at an angle to the circumference with $\frac{1}{4}$ -orbital misalignment angles. The π -orbital alignment is almost perfect in fullerene, whereas this is not the case for carbon nanotubes. The π -orbital misalignment angles are the main source of strain in the carbon nanotubes, and they represent a clear contrast with fullerene chemistry. Pyramidalization angles and π -orbital misalignment angles of SWCNTs scale inversely with the diameter of the nanotube, so a differentiation of CNT reactivity is expected for CNTs with different diameter [9].

9.4 Properties of CNTs

9.4.1 Surface properties

As was said above, the tips and the walls have different electrical and physical properties. The walls are highly

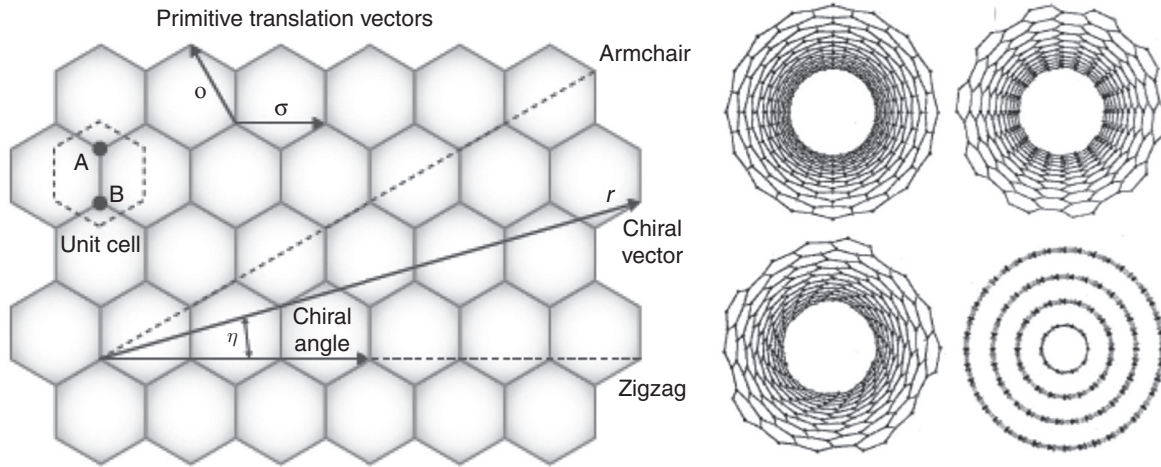


Figure 9.1 On the left: the honeycomb lattice of graphene. The chiral vector is given by \mathbf{L} , and the chiral angle is given by η . Reprinted from Ando 2009 [11]. On the right: models of differently wrapped sheets of graphene, depending on η . Reprinted from Bonard et al. 2001 [59].

hydrophobic, and that is why the tubes have the tendency to coagulate in aqueous solutions; the ends, instead, often terminate with oxygenated species, which confer hydrophilic properties and electrochemically behave as the edge plane bands. Because of this behavior, carbon nanotubes are often dispersed in non-polar organic solvents, or with the use of surfactants or polymer solutions.

As said before, the homogeneity of the CNT surface strongly depends on the synthesis techniques and post-synthesis treatments. High-temperature methods, for example, lead to almost perfect periodic honeycomb structures, while low-temperature synthesis causes defects in the nanotube walls. For example, carbon rings can present pentagons or heptagons instead of hexagons, and the presence of these can change the local curvature of the nanotube surface. In the same manner, hemispheric or conical ends can form at the CNT tip if pentagons are present instead of hexagons.

Carbon atoms located in the defects are more reactive than those in hexagonal conformation, and can form complexes with chemical groups that can be exploited to alter the surface properties of the CNT. The introduction of oxygen-based groups on the CNT surface is one of the most common. Of the possible functional groups, carboxylic groups ($-\text{COOH}$) exhibit favorable electrochemical properties: Chou *et al.* demonstrated that CNT electrochemistry and rate of electron transfer are dominated by oxygen-based species at the tips rather than pure carbon structure [10].

9.4.2 Electronic properties

As mentioned above, SWCNTs can behave as metals, semiconductors, or small-bandgap semiconductors, depending on their chirality, diameter, and the quantity and type of impurities present in the tubes. A SWCNT is a seamless rolled sheet of graphene wrapped either along one of the

symmetry axes (Figure 9.1), or in such a way that each unit cell is aligned on a spiral. Zooming on the honeycomb lattice structure of the graphene, it is possible to introduce the vector \mathbf{L} , which is the chiral vector, whereas η is called the chiral angle. A schematic of the vector and angle is illustrated in Figure 9.1. The chiral vector can be described by its primitive translation vectors:

$$\mathbf{L} = n\mathbf{a} + m\mathbf{b}$$

Therefore, the structure of the nanotube can be described by the set of integers \mathbf{a} and \mathbf{b} . As an example, zigzag nanotubes have $\eta = 0$, while “armchair” tubes have $\eta = \pi/6$.

Tubes with different η angles are generally called chiral tubes. The (n, m) indices univocally define the chirality and the diameter of the SWCNTs, and thus also the electronic properties.

If $n - m = 3q$, where q is an integer, then the SWCNT is metallic. Otherwise, if $n - m \neq 3q$, then it is semiconducting. About two-thirds of all the SWCNTs are semiconductive [11],[12]. The electronic structure of a SWCNT can be derived from that of graphite. Energy bands near the Fermi level for the graphene structure are depicted in Figure 9.2.

The conduction and the valence bands intersect in six corners of the Brillouin zone, called Dirac points (K points). It can be demonstrated that the energy bands of SWCNTs are a set of 1D cross-sections of those for 2D graphite. N pairs of 1D energy dispersion relations are obtained, where N is the number of hexagons per unit cell. N can be obtained as a function of n and m as:

$$N = \frac{\mathbf{L} \times \mathbf{T} 2(m^2 + n^2 + mn)}{\mathbf{a} \times \mathbf{b} d_r} = \frac{2l^2}{a^2 d_r}$$

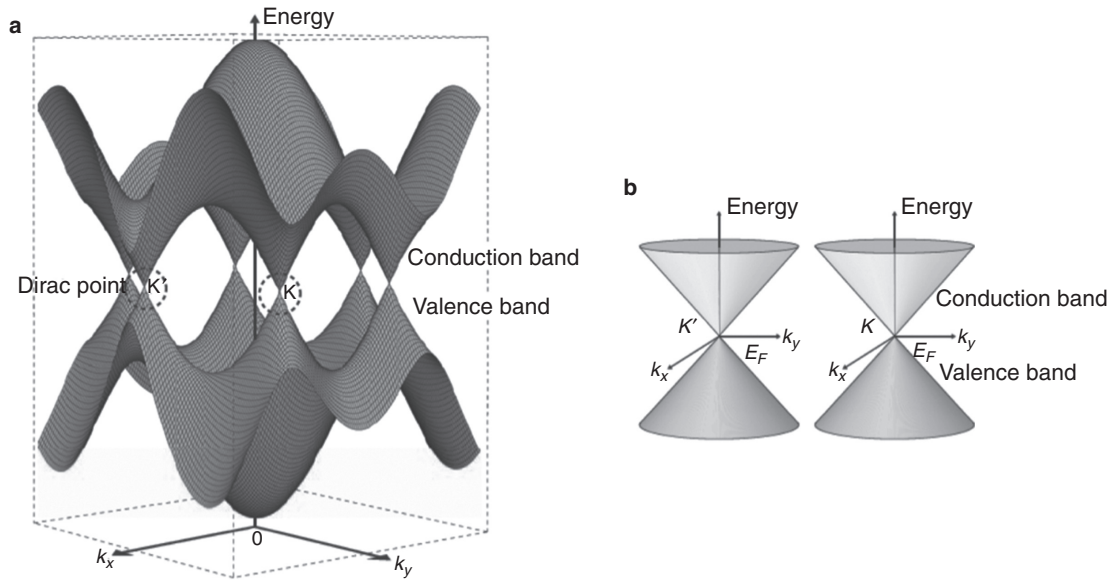


Figure 9.2 Energy bands near the Fermi level in graphene. Reprinted from Ando 2009 [11].

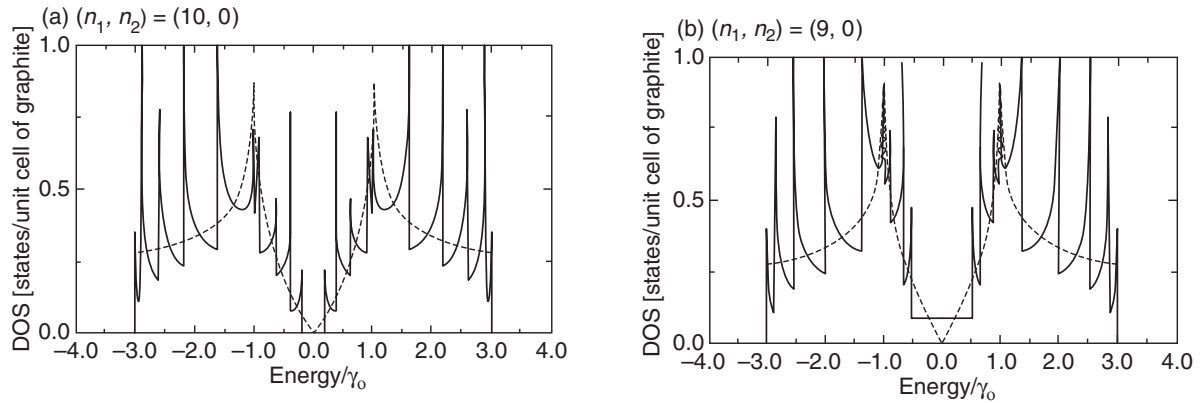


Figure 9.3 Density of states per unit cell for carbon nanotubes with metallic (a) and semiconducting (b) behaviors. The dotted line refers to the DOS of graphene. Reprinted from Saito et al. (1998) [13].

where \mathbf{T} is the translation vector which is parallel to the nanotube axis and normal to \mathbf{L} , l is the circumferential length of the nanotube, and d_t is the greatest common divisor of $(2m+n)$ and $(2n+m)$. As already mentioned, the N pair of energy dispersion curves correspond to the cross-sections of the 2D energy dispersion surface, where cuts are made at a fixed distance depending on the lattice vectors in the reciprocal space. So if, for a given (n, m) nanotube, the cutting line passes through one of the K points depicted in Figure 9.2, then the 1D energy bands have a zero energy gap. Moreover, the density of states (DOS) at the Fermi level has a finite value, meaning that such carbon nanotubes are metallic. On the other side, if the cutting line does not pass through a K point, then the carbon nanotube behaves as a semiconductor,

with a finite energy gap between the valence and the conduction band [13].

Figure 9.3 compares the density of states for metallic (9,0) and semiconducting (10,0) nanotubes. It is interesting to notice that near the Fermi level, located at $E=0$, semiconducting nanotubes show a null value, whereas metallic nanotubes have non-zero value. In particular, the energy gap (E_g) of semiconductive nanotubes is inversely proportional to the nanotube diameter (d_t)

$$E_g = \frac{|t|a_{C-C}}{d_t}$$

where $|t|$ is the nearest neighbor C-C tight binding overlap energy and a_{C-C} is the nearest neighbor C-C distance on a graphene sheet. Moreover, carbon nanotube DOS shows

several discontinuities, called singularities, that are absent in graphene DOS [13].

9.4.3 Transport properties

As mentioned in the previous section, the electronic structure of SWCNTs depends both on the orientation of the honeycomb lattice with respect to the tube axis and on the radius of curvature of the graphene sheet. In the case of MWCNTs, the electronic conduction takes place essentially through the external tube, even if the interaction among internal sheets may affect the electronic properties. Energy dispersion curves can also vary owing to the application of a stress to the tube. This is particularly important for carbon nanotube-based composites, when both mechanical and electronic properties have to be taken into account. The conduction of charge carriers in metallic SWCNTs is thought to be ballistic, independent of the nanotube length. The electric conductance is predicted to be twice the fundamental conductance, owing to the existence of two propagating modes. Because of the reduced scattering, current densities up to 109 A/cm^2 can be transported without damage. Such values are three orders of magnitude higher than in copper. In the case of defects, electrons often localize and charge transport is dominated by tunneling effects.

9.4.4 Electrochemical properties

In general, CNTs contain two kinds of carbon atoms: the tips behave like the edge plane of highly oriented pyrolytic graphite, while the sidewalls resemble the basal plane of highly oriented pyrolytic graphite.

Electrochemical enhancements can be correlated with the length of the nanotubes and the presence of oxygenated groups at the tips. For example, Li *et al.* observed that in cyclic voltammetry of ferricyanide, the peak current was proportional to the length of the tubes [14]. Moreover, a faster rate of electron transfer could be attributed to the oxygenated ends, apparently allowing a more efficient electron transfer than in edge planes of pyrolytic graphite. This validates the hypothesis that electron transfer occurs predominantly at sites where oxygenated species exist.

The conductivity of nanotubes can be increased by doping. In addition to creating functional groups, acid treatment can result in ion penetration into the centers of the tubes and the alteration of their electronic properties by injecting electrons or holes into the valence or conduction bands of the tubes. Therefore, the electrochemical properties of a nanotube are sensitive to its pre-treatment and purification. Many studies have reported remarkably high electrode capacitances, clearly seen from the large separation of the baselines between the anodic and the cathodic scans in cyclic voltammetry. Azamian *et al.* showed that the capacitance of SWCNT paper electrodes is three to four orders of magnitude

higher than for other carbon electrodes [15]. They divided the capacitive effect into a fast process and a slow process. The fast process is due to the charge of the electrical double layer, whereas the slow process appears to be a pseudo-capacitance related to surface Faradaic reactions of redox active oxides. Surface oxides produce distinct redox peaks, which contribute to the apparent capacitance. Electrodes based on carbon nanotubes show peak-shaped voltammograms like macroscopic electrodes, despite the potential for each nanotube to act as a nanoelectrode. In most cases CNT density is sufficiently high for significant overlap of the diffusion layers to each nanotube, such that the overall diffusion layer approximates to linear diffusion. However, Taurino *et al.* pointed out that horizontal CNTs show a cyclic voltammogram more sigmoidal in shape, similar to a nanoelectrode ensemble [16].

9.5 Strategies to develop CNT-based biosensors

The application of electrodes modified with carbon nanotubes leads to a novel type of electrochemistry, where the favorable electrochemical properties of CNTs can be exploited to enhance sensor performance in terms of sensitivity and detection limit. Such interesting properties can be also combined with the nanoscale dimension of CNTs, which makes them ideal for interacting with biomolecules and proteins. One of the main problems when handling CNTs is their tendency to aggregate together in aqueous solutions, owing to the intrinsic hydrophobicity of the sidewalls and the van der Waals forces between the tubes. Therefore, it is quite difficult to obtain homogeneous CNT solutions or composites. On the other hand, owing to their interesting electrochemical properties, several strategies have been proposed for the immobilization of CNTs on electrodes. For example, covalent and non-covalent functionalizations are by far the most common strategies for solubilizing and manipulating CNTs. The following section gives an overview of the main strategies for the preparation of CNT-based electrodes.

9.5.1 Drop casting of random distributed CNTs

The most straightforward strategy to modify electrodes with carbon nanotubes is by drop casting. A drop of the CNT dispersion can be cast onto the surface and let dry before electrode use. So, the main issues to achieve homogeneous modification are CNT solubility, to obtain a well-dispersed solution; solvent volatility, to avoid residuals after the drying step; and solvent chemical inactivity, to avoid interference with the electrochemical measurement. Different types of solutions have been proposed for glassy carbon and gold electrodes. Some researchers have reported the dispersion of MWCNTs in acids. In particular, Wang and co-workers developed modified glassy carbon electrodes by dispersing MWCNTs in a solution of concentrated sulfuric acid in one case [17] and

concentrated nitric acid in another case [18]. The electrodes were allowed to dry at 200 °C for 3 h in [17], and at room temperature for 30 min in [18]. Surfactants such as dihexadecyl hydrogen phosphate (DHP) [19] and sodium dodecyl sulfate (SDS) [20] have also been proposed as dispersing agents for MWCNTs. The dispersion in organic solvents has so far driven the research in most of the literature. CNT powder was dispersed in polar solvents such as acetonitrile [21], which can dry in air at room temperature, and dimethylformamide [22], which can be dried under an infrared lamp. Non-polar solvents, such as bromoform, have also been proposed for the detection of dopamine [23]. Chloroform is another type of non-polar solvent often used to disperse MWCNTs, as it evaporates quickly at room temperature leaving the MWCNT attached to the electrode surface [24].

9.5.2 Aligned CNTs

As mentioned previously, chemical vapor deposition allows the growth of aligned CNTs [25]. An example of vertically aligned MWCNTs is depicted in Figure 9.4.

The growth can be performed directly onto a silicon wafer, so CNTs are used as pure electrodes, coupled with conductive paints or pastes to guarantee the connections. Otherwise, they can be transferred to a metallic substrate after the growth process [26]. Alternatively, nanotube functionalization with thiol groups permits CNTs to be aligned on a gold surface by self-assembly [27]. Most of the literature on CNTs used for biosensing is based on the assumption that tips are responsible for their electrochemical activity. Gooding *et al.* investigated the electron-transfer properties of redox enzymes attached to the end of aligned SWCNTs [28]. They found that the rate constant for

electron transfer for the redox enzyme on top of the aligned carbon nanotubes was similar to that for redox enzymes directly attached to a modified gold electrode. The tips of SWCNTs do not add any significant electrical resistance.

9.5.3 CNT-paste electrodes

CNT-paste electrodes are typically manufactured by hand-mixing CNT powder with mineral oil to obtain a homogeneous paste. The paste can then be packed into a micro-cavity connected with an electrical conductor, and used as a working electrode [29]. The development of CNT-paste electrodes opens the opportunity to new strategies for the fabrication of electrodes. CNT-paste can also be used as an ink to prepare screen-printed electrodes. Wang *et al.* showed that the ink that they developed, deposited on alumina ceramic plates, has a microporous structure of flake-shaped particles, non-uniformly distributed [30].

9.5.4 CNT-polymer nanocomposite electrodes

Conductive polymers such as polypyrrole (PPy) and polyaniline (PAn) have been used in the preparation of CNT-polymer nanocomposites. Gao *et al.* grew an aligned carbon nanotube array on a quartz substrate by CVD [31]. Separately, pyrrole monomers were electrochemically oxidized in buffer solution containing glucose oxidase (GOD), and the resulting mixture was used for uniformly coating the aligned CNTs. The developed biosensor was used to detect glucose concentration up to 8 mM. PAn was also used in a CNT-based composite for the immobilization of cholesterol oxidase by the electrophoretic technique. The

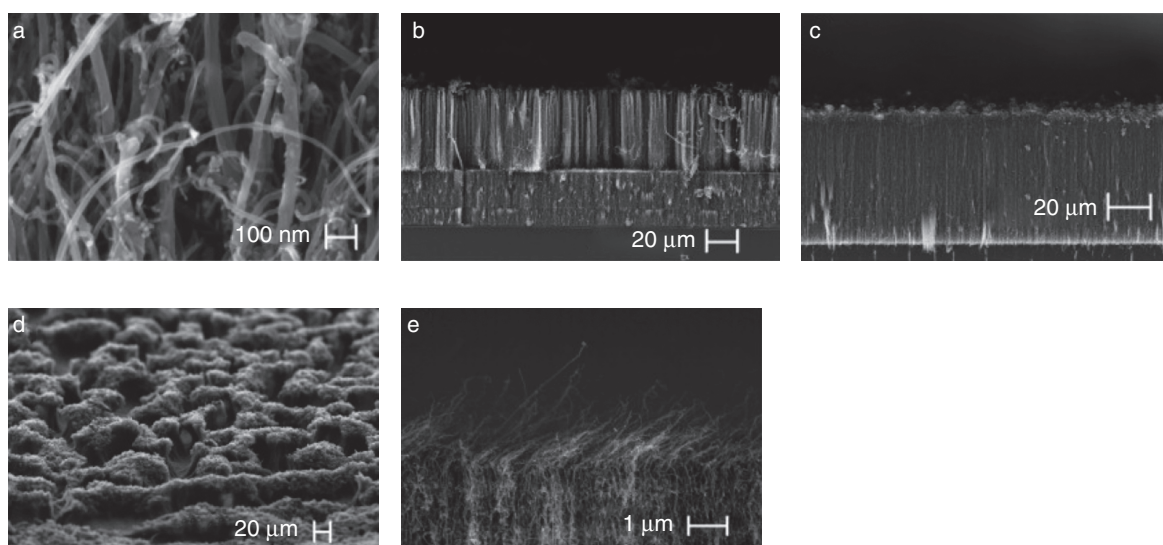


Figure 9.4 Field-enhanced SEM of vertically aligned CNT, reprinted from Taurino *et al.* (2011a) [16].

colloidal suspension of PAN-MWCNTs was electrophoretically deposited to form a uniform film on an ITO-coated glass plate, and cholesterol oxidase was then covalently immobilized on the composite film via amide bond formation [32].

A different approach was proposed by Wang *et al.* in which Nafion was used as the solvent for well-dispersed CNT solutions [33]. Nafion is a perfluorinated ionomer widely used to confine electrocatalysts and biomolecules on electrode surface. The difference between PPy or PAN and Nafion is that the latter is an insulating polymer instead of being conductive. However, Wang demonstrated that it has excellent capability to solubilize the CNTs and confine them onto the electrode surface. An example of MWCNTs dispersed in a Nafion matrix together with GOD is reported by Tsai *et al.* [34].

Chitosan is a natural biopolymer with excellent properties such as biocompatibility, film-forming ability, non-toxicity, affinity with proteins, and good adhesion to the chemically modified fabrication. CNTs can be well-dispersed in chitosan and easily form a uniform film on glassy carbon electrodes. Therefore, chitosan has been extensively used for CNT entrapment [35].

9.5.5 Layer-by-layer assembly of CNTs

The layer-by-layer method is based on the alternate adsorption of oppositely charged species from their solution. In the case of CNTs, negatively charged oxygenated groups can be exploited by pairing them with positively charged layers to assemble a CNT-based composite. This procedure gives uniform and homogeneous CNT multilayer films with highly controlled physical and mechanical properties. Several layers can be immobilized by simply repeating the procedure, and the number of layers can be optimized to obtain the best performance of the biosensor. Deng *et al.* [36] described the immobilization of CNTs by assembling alternate layers of cationic poly(ethylenimine) (PEI) layers and glucose oxidase. As another example, Wang *et al.* used poly(diallyldimethylammoniumchloride) (PDDA) as highly positively charged polymer to disperse SWCNTs. GOD was then adsorbed on PDDA to form a multilayer film on Pt electrodes [37]. The authors performed an optimization of the biosensor sensitivity according to the number of deposited layers, finding that seven layers were optimal for this particular example.

9.6 Carbon nanotubes and biocompatibility aspects

Despite their fundamental role in enhancing biosensor performance, the real implementation of CNTs in biomedical devices relies on the outcome of studies on their toxicity. CNT toxicity may arise from their dual nature of nanoparticle and nanofiber: on the one hand, the large surface area/

mass ratio of a CNT increases the probability of interaction with a cell, and confers great capacity for adsorption, transport, and uptake of toxic substances in the body; on the other hand, the nanotube length may induce foreign body reactions, since longer fibers (>17 μm) are difficult to phagocytize [38]. To date, information related to CNT safety is contradictory, and present results indicate both toxicity and inertness of these nanomaterials. Good reviews of experiments concerning the safety of carbon nanotubes are given in [38],[39].

The picture emerging from the literature is that CNT toxicity is dependent on many factors including purity, aggregation status, dimensions, coating or functionalization, cell type, and bioassay technique. In general, experiments confirmed that:

- Unrefined CNT, owing to the presence of transition metal catalysts and other impurities derived by their synthesis, are cytotoxic.
- Pristine CNTs cause minimal *in vitro* and *in vivo* toxicity, but only when they accumulate in cells at high concentrations.
- The aggregation of CNTs in fibers is critical in determining their toxicity. Efficient dispersion techniques, such as covalent binding or electrostatic adsorption of peptides, acids, amines, and polymers, seems to prevent their aggregation, and non-aggregated fibers do not show significant toxicity effects.
- CNTs immobilized on a substrate or embedded in a nanocomposite are not toxic, although the degradation of the matrix can produce particles that cause dose-dependent adverse effects on cells.

According to these findings, from the perspective of an implantable biosensor, the use of short, functionalized CNTs immobilized in a nanocomposite may represent a safe implementation. However, it is important to say that, to date, owing to the novelty of this material, there are no exhaustive studies concerning the long-term effects of CNTs in living organisms or the impact of these substances on the environment.

9.7 Applications

9.7.1 An example: P450-biosensors for drug detection

Cytochromes P450 (abbreviated as P450s or CYPs) are a large group of enzymes involved in the metabolism of over 1 000 000 different xenobiotic and endogenous compounds [40]. Depending on the organism, they contribute to vital processes including carbon source assimilation, biosynthesis of hormones and/or structural component of cells, and carcinogenesis and degradation of xenobiotics [41]. More importantly, CYPs are the major enzymes involved in human drug metabolism and bioactivation, accounting for about 75% of the total number of different metabolic reactions (Figure 9.5) [42]. In humans, just five P450 isoforms

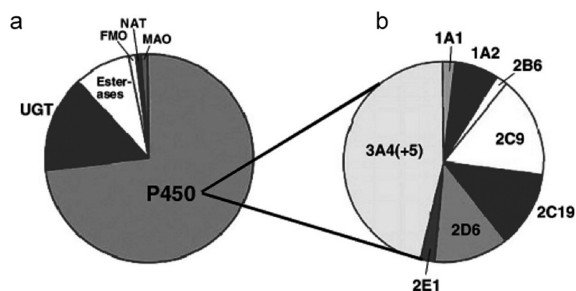


Figure 9.5 Contribution of enzymes to the metabolism of marketed drugs. (a) Fraction of human enzymes involved in human metabolism: FMO, flavin containing monooxygenase, NAT, N-acetyltransferase, MAO, monoamine oxidase. (b) P450 isoform contribution to drug metabolism. Reprinted from Guengerich (2007) [42].

are responsible for the metabolisms of 95% of known pharmacological compounds [43]; this makes the CYPs promising candidates for the construction of biosensors for therapeutic drug monitoring. In principle, a sensor platform bearing all five of these cytochromes on different sensors could be used to follow the drug response of individuals in almost every kind of pharmacological treatment.

The most common reaction catalyzed by the P450s is the insertion of an oxygen atom into a substrate (RH), as shown in the equation below.



The biological significance of this reaction, called *monooxygenation*, is to transform liposoluble compounds into hydrosoluble, in order to be easily excreted with the urine.

The vast majority of P450s require additional proteins and cofactors components to supply the electrons needed in the monooxygenation reaction: human cytochromes, for example, rely on two additional proteins: P450 reductase, cytochrome B5 reductase, and the cofactor NADPH.

P450 biosensors measure the electron transfer between protein and electrode: proteins are immobilized on the electrode surface, and the electrons needed for the monooxygenation reaction are directly supplied by the electrode, without the need to employ additional proteins. Electron demand depends on the activity of the enzyme and is correlated to the substrate concentration at the electrode interface. Ideally, higher concentrations of substrate will increase the electrons needed, and therefore will generate higher currents.

The different nature of substrates bound to the cytochrome will change the energy required for activating the electron transfer, and therefore the potential at which this reaction will take place [44]. The need to query the cytochrome response at different potentials makes the voltammetric techniques the ideal choice for P450-based detection.

Voltammetry is the study of current as a function of applied potential. In cyclic voltammetry, the potential is swept back and forth at a constant rate between two extreme values, and the actual current value is measured as the dependent variable. The total current in the cell is the difference between the **oxidative current**, generated by the potential sweep towards more positive values, and of the **reductive current**, produced when the potential is swept back to more negative values. The behavior of the current as a function of the applied potential is described by the Butler–Volmer equation:

$$I = I_{\text{ox}} - I_{\text{red}} = nFAk_0 \left\{ [O]_{0,t} e^{\frac{-\alpha F(E - E_{\text{eq}})}{RT}} - [R]_{0,t} e^{\frac{-\alpha F(E - E_{\text{eq}})}{RT}} \right\}$$

where I is the net current of the cell, I_{ox} and I_{red} are respectively the absolute values of the oxidation and the reduction current, E is the applied potential, E_{eq} the equilibrium potential, F the Faraday constant, R the universal gas constant, T the absolute temperature, n the electrons exchanged in the redox, and A the electroactive area. $[O]$ and $[R]$ are the oxidized and reduced forms of the same species. The constant k_0 is a measure of the redox efficiency: small values of k_0 indicate very slow redox processes. The parameter α is the charge transfer coefficient.

The current generated during the potential scan is the sum of two components: capacitive and faradic. The *capacitive current* originates when solution electrolytes become polarized and migrate to the electrode bearing opposite charge. The accumulation of charged ions at the interface generates an electrical double layer that behaves like a capacitor with area equivalent to the electroactive surface. The capacitive current i_c is defined as:

$$i_c = C \frac{dE}{dt} = Cv$$

where C is the capacitance of the electrical double layer, E the applied potential, t the time, and v the scan rate. In voltammetric analysis, the capacitive current is considered non-specific background interference and must be subtracted from the total current to obtain the faradic contribution. In cases where the concentration of the electroactive compound is too low, or when the scan rate is too high, the faradic current can be masked by the capacitive current causing problems in the detection.

The *faradic current* is due to the electron transfer at the electrode interface, and represents the current of interest for the electrochemical detection. In steady state conditions, the faradic current assumes a peak shape with the current maximum centered on the formal potential of the analyte [45]. In a backward potential sweep of a soluble electroactive species, when the electrode potential approaches the specimen's formal redox potential, the reduction of the analyte begins, and current starts to flow. As the potential continues to grow

more negative, the surface concentration of the species drops; hence, the flux to the surface (and the current) increases. At the formal redox potential, the current intensity is defined by the Randles-Sevcik equation:

$$i_p = 0.4463nFAC \left(\frac{nFvD}{RT} \right)^{\frac{1}{2}}$$

where i_p is the peak current, C the analyte concentration, D the diffusion coefficient of the analyte, A the electrode area, F the Farad constant, T the temperature, R the gas constant, v the voltage scan-rate, and n the number of electrons involved in the redox. As the potential crosses the reduction potential peak, surface concentration drops nearly to zero, mass transfer reaches a maximum rate at the surface, and then declines as the depletion effect sets in. This is the case where the current is limited by the diffusion of the reagents to the electrode surface. When the potential is swept in the opposite direction, symmetric mechanisms take place and the whole reduced species is oxidized again.

The P450 biosensors rely on a technique called catalytic protein film cyclic voltammetry [46]. In the absence of substrate and at sufficiently high coverage, a redox enzyme immobilized onto an electrode gives peak-like signals resulting from the reversible transformation of its redox centers. The potential sweeping in cyclic voltammetry is used to artificially turn “on” and “off” the redox center of the enzyme (Figure 9.6).

We previously said that the P450 active site needs two electrons to perform the monooxygenation reaction. In a P450 biosensor, these electrons are artificially provided by the electrode when sufficient energy for the electron transfer is furnished. In absence of substrate, this current flow will continue until all the proteins immobilized have their

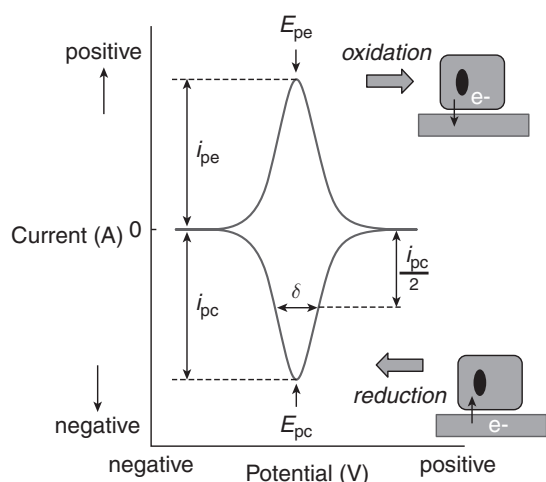


Figure 9.6 Cyclic voltammetry response from a film of adsorbed protein containing a single redox active center undergoing reversible electron transfer. E_p , peak potential.

substrate reduced (enzyme “on”). As a result, a peak-shaped Faradic current is generated. Ideally, a potential sweep in the opposite direction will regenerate the active site producing a symmetrical peak (enzyme “off”). During the catalysis, the electrons of the active site are further transferred to the substrate, allowing the heme to accept new electrons from the electrode and producing a Faradic contribution known as *catalytic current*. Cyclic voltammetry of the catalytic protein film establishes a relationship between current, enzyme concentration, and substrate concentration:

- The detected faradic current is associated only with the electron transfer between enzyme and electrode. The substrate is not electroactive.
- Higher amounts of enzyme immobilized (electroactive coverage) allow the conversion of a bigger number of substrates in a given period of time, leading to higher catalytic currents.
- The demand for electrons in presence of substrate is directly related to the speed of the enzymatic catalysis and is therefore dependent on the enzyme kinetics: when the substrate concentration at the interface is much lower than the enzyme concentration, the reaction speed (and therefore the generated current) is proportional to the substrate concentration. Conversely, if the concentration of substrate at the interface is bigger than the enzyme concentration, the enzymatic speed (and therefore the current generated) reaches a maximum, making it impossible to establish a relationship with the substrate concentration.
- The electron demand also depends on the substrate diffusion to the electrode. When a fixed substrate concentration is supplied at a constant rate and products do not accumulate at the electrode interface, the catalytic current takes the shape of a wave. The wave shape can be achieved by controlling diffusion at the interface with rotating disk electrodes or with microelectrodes. The absence of diffusion control will lead to peak-shaped catalytic currents.

Some of the main issues concerning the P450 biosensors are the poor stability of the protein and the low efficiency of electron transfer between protein and electrode.

The use of P450 microsomes can solve the first problem. A microsome is a construct obtained during the artificial disruption of cells. The endoplasmic reticulum with the associated proteins (P450, CPR, cytochrome b5) is fragmented and recombined in vesicles that can be isolated by centrifugation. Casting microsomes onto an electrode surface provides a physiological environment for the P450 and improves its stability.

General guidelines to improve the direct electron transfer between protein and electrode include that the electron transfer distance between the redox protein and the electrode surface has to be as short as possible, or at least that the electrode architecture should have predefined electron

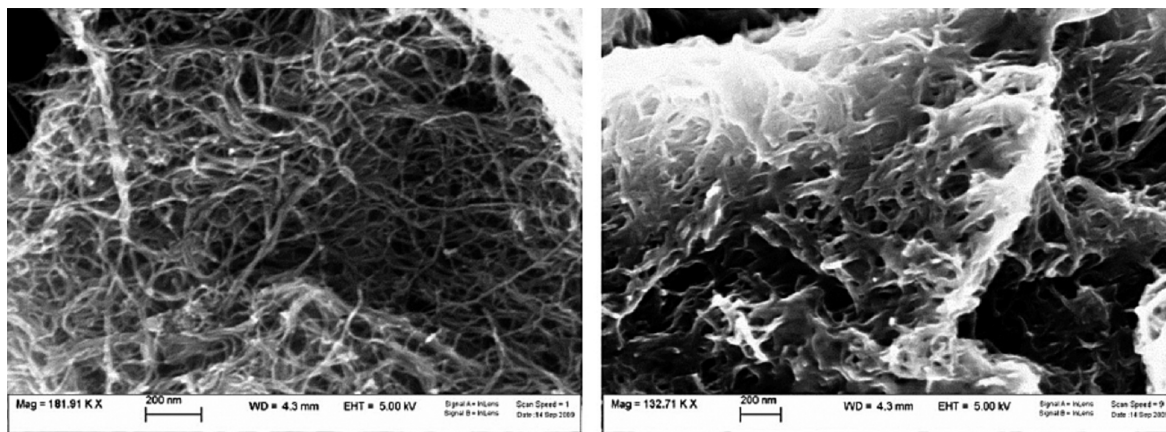


Figure 9.7 SEM images of working electrode nanostructured with MWCNT (left) and MWCNT plus P450 microsomes (right).

transfer-pathways interconnecting the redox site within the enzyme and the electrode surface; the protein should be directly adsorbed on the electrode surface and should be working, avoiding denaturation by the enzymes; the proteins should be adsorbed as a monolayer, since they limit the electron transfer-pathway for further protein layers lying on top. Drop casting of carbon nanotubes onto an electrode surface can satisfy many of these guidelines.

Figure 9.7 shows a scanning electron micrograph of an electrode treated with drop-cast nanotubes (left). The nanotubes appear randomly organized in a tridimensional conductive net that greatly increases the electrode surface. On the right, the same structure after the deposition of P450 microsomes is presented. The CNT net is still visible, but fibers are thickened, presenting a value on average 8 nm thicker than the bare MWCNT [47].

Considering that the average diameter of microsomes varies between 50 and 150 nm [48], the slight thickness increase indicates a rupture of the microsomes and the formation of a lipid/protein monolayer around the nanotube. It is therefore possible to conclude that the microsomes establish strong hydrophobic interactions with the CNT, leading to the formation of a lipid/protein monolayer around the CNT surface.

The addition of CNT and the intimate contact with the protein has several significant benefits:

1. Since CNTs and P450 possess similar dimensions, enzyme adsorption can occur without significant loss of enzyme shape or catalytic activity [49].
2. The CNT nanostructuring provides a third dimension available for the enzyme immobilization. The increased electroactive coverage allows the conversion of a greater number of substrates in a given period of time, leading to higher catalytic currents; moreover, the porous nature of the nanostructure allows deeper penetration of the electrolytes solution and a larger surface available for the redox reaction.

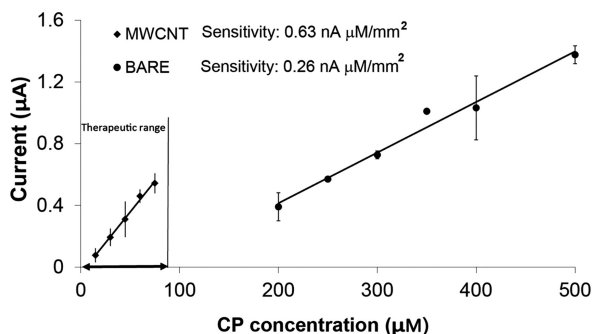


Figure 9.8 Cyclophosphamide calibration curves obtained from bare and MWCNT-nanostructured electrodes. Values reported are normalized to the P450 residual current. Error bars: average of three measurements. Image adapted from Carrara et al. (2011) [47].

3. Physical adsorption of the enzymes onto CNT enables direct electron transfer between the electrode and the active site, minimizing the electron tunneling distance [50].
4. Functionalization of the sidewall and tips with carboxylic groups provides reactive sites that improve the electron transfer rate between active site and electrode [10].

The better performance of P450 enhanced by CNTs is shown in Figure 9.8, which shows a calibration curve for the antitumor compound cyclophosphamide obtained using a CYP3A4 biosensor.

When P450 is immobilized onto bare electrodes, significant current responses were obtained only at high drug concentrations. The best detection limit achieved with bare electrodes was 56 μM. Such behavior is unacceptable for practical applications, since the cyclophosphamide concentration range in conventional therapies, the so-called therapeutic range, has been calculated to vary from 2.6 μM to 76.6 μM [51]. On the other hand, when electrodes

are nanostructured with CNT, a 2.4-fold sensitivity increase and a detection limit of 12 μM can be achieved, which allows drug detection in the therapeutic range. A sensitivity increase due to MWCNT nanostructuring has been reported for similar concentration ranges, and it has been shown for several drugs and different P450 isoforms as well as biosensors based on oxidases for the detection of glucose, lactate, glutamate, and ATP [24],[35],[47],[52–55].

P450 biosensors enhanced by carbon nanotubes have also proved useful for the detection of compound in biological fluids such as serum, as reported in [47]. The possibility to detect drugs in plasma in their therapeutic range represents an important step towards the realization of biosensors for real-life applications, since one of the biggest obstacles to overcome in drug detection is the capability to sense compounds in complex media, with concentrations typically in the order of micro- or nanomoles.

9.7.2 Therapeutic drug monitoring

Therapeutic drug monitoring (TDM) is a multi-disciplinary clinical specialty aimed at improving patient care by individually adjusting the dose of drugs for which clinical experience or clinical trials have shown this to improve outcome in general or special populations.

TDM is requested as an aid for the manipulation of the current medication regimen for patients who are unresponsive to a given therapy; in cases of suspected toxicity; to assess compliance with the medication regimen; or when the clinical status of the patient is changed [56]. This last point is of particular interest, as many of the drugs that are monitored therapeutically are taken for a lifetime and must be maintained at steady concentrations year after year while the patient ages and goes through life events such as pregnancies, temporary illnesses, infections, emotional and physical stresses, accidents, and surgeries. Over time, patients may acquire other chronic conditions that also require lifetime medications which may affect the processing of their monitored drugs. Examples include cancer, cardiovascular disease, kidney disease, thyroid disease, liver disease, and HIV/AIDS.

At present, routine therapeutic drug monitoring procedures have been established for compounds with narrow therapeutic index and high interpatient pharmacokinetic variability [56], [57]. These include antifungal, antiretroviral, anticonvulsant and immunosuppressant drugs, theophylline, aminoglycosides, and psychotropic drugs [58]. After the request is assessed, sampling, analysis and interpretation of results should be ideally reported within a single working day in order to ensure a quick and safe regimen optimization. Drug concentration results are interpreted by a team of experts on the basis of patient-related and drug-related variables and then finally sent to the physician who can decide eventual modifications to the therapeutic regime.

Despite the advantages of TDM, its use has been limited to few patients and only to a few indications [57]. This is for the following reasons:

- **Technology:** Current analytical techniques which grant drug sensing with sufficient accuracy, specificity selectivity and reproducibility require highly trained personnel and specific equipment. Analysis is therefore carried out by few laboratories, at high costs, and at the expense of a longer time lag between TDM request and reporting of results. Examples of analytical techniques include various forms of chromatography, mass spectroscopy, and immunoassays. Although high-throughput technologies have become available in the last few years enabling faster reporting of results, sampling and analysis is still carried out in specific centers.
- **Knowledge:** A reason for the lack of TDM is the absence of sufficient information regarding a drug's pharmacokinetic or pharmacodynamic data and its therapeutic ranges. Implementation of TDM procedures in preclinical and clinical drug development, as well as in pharmacovigilance, can give earlier insight into drug-related and patient-related variables enabling the development of more specific compounds, and more personalized therapy [56]. Examples of information relevant to pharmacological research obtained from TDM include the discovery of poor and ultrafast metabolizers, as well as the discovery of accidental drug interactions [57].
- **Human error:** It has been estimated that about 20% of therapeutic adjustments following TDM of antidepressants were previously incorrect [57]. Most of the reasons can be attributed to human errors. Drugs must be sampled at steady state; time of dose administration, dosage regimen as well as time and frequency of blood sampling must be carefully planned and recorded in order to reconstruct the correct pharmacokinetic profile [56],[58]. Errors are proportional to the number of samplings performed; repetitive manual data handling represents an additional source of errors in diagnosis, as omissions and confusion can happen.

Given these considerations, the introduction of P450 biosensors could benefit TDM practice by improving practice, subject compliance, and pharmaceutical research:

- **Diffusion.** P450 biosensors can be designed to be small, cheap, and easy to use. Moreover, electrochemical biosensors provide an immediate reading of the substance of interest. Cost reduction and simplicity of use may allow the diffusion of TDM tests from a small number of specialized laboratories to a bigger number of medical centers or even the patient's house.
- **Compliance.** The introduction of biosensors can improve the compliance of both patients and operators. Home testing can both simplify the life of patients and reduce the cost of hospitalization. The development of automatic sampling

procedures and remote data transmission can reduce human error during analysis and data manipulation. An electronic device can automatically collect relevant information regarding patient status, testing procedure and analyses results, and send the data directly to a specialized center for clinical interpretation. Ideally a patient can self-test at home and receive new therapeutic indications online. Additionally, the diffusion of long-term implantable biosensors can benefit patients with chronic pathologies for which frequent control of drug pharmacokinetics may be essential. In this respect, elderly people, more subject to ageing effects and to the insurgence of chronic pathologies, represent a potential target.

- **Research.** The diffusion of inexpensive TDM procedures and automatic data collection can help in discovering unknown drug interactions; pharmacokinetic and pharmacodynamic data obtained from TDM can be classified and used to predict therapeutic outcomes in new patients with similar clinical history, or in the design of new compounds.

References

- [1] Iijima, S., 1991. Helical microtubules of graphitic carbon. *Nature* **354**(6348), 56–58.
- [2] Kroto, H.W., Heath, J.R., O'Brien, S.C., Curl, R.F., Smalley, R.E., 1985. C 60: buckminsterfullerene. *Nature* **318**(6042), 162–163.
- [3] Gooding, J.J., 2005. Nanostructuring electrodes with carbon nanotubes: A review on electrochemistry and applications for sensing. *Electrochimica Acta* **50**(15), 3049–3060.
- [4] Krupke, R., Hennrich, F., Löhneysen, H.v., Kappes, M.M., 2003. Separation of metallic from semiconducting single-walled carbon nanotubes. *Science* **301**(5631), 344–347.
- [5] Chattopadhyay, D., Galeska, I., Papadimitrakopoulos, F., 2003. A route for bulk separation of semiconducting from metallic single-wall carbon nanotubes. *Journal of the American Chemical Society* **125**(11), 3370–3375.
- [6] Gong, K., Yan, Y., Zhang, M., *et al.* 2005. Electrochemistry and electroanalytical applications of carbon nanotubes: a review. *Analytical Sciences* **21**(12), 1383–1393.
- [7] Wong, H-S.P., Akinwande, D., *Carbon Nanotube and Graphene Device Physics*. Cambridge University Press, 2010.
- [8] Dai, H., 2002. Carbon nanotubes: synthesis, integration, and properties. *Accounts of Chemical Research* **35**(12), 1035–1044.
- [9] Niyogi, S., Hamon, M., Hu, H., *et al.* 2002. Chemistry of single-walled carbon nanotubes. *Accounts of Chemical Research* **35**(12), 1105–1113.
- [10] Chou, A., Böcking, T., Singh, N.K., Gooding, J.J., 2005. Demonstration of the importance of oxygenated species at the ends of carbon nanotubes for their favourable electrochemical properties. *Chemical Communications* **7**, 842–844.
- [11] Ando, T., 2009. The electronic properties of graphene and carbon nanotubes. *NPG Asia Materials* **1**(1), 17–21.
- [12] Harris, P.J., *Carbon Nanotubes and Related Structures*. Cambridge University Press, 2001.
- [13] Saito, R., Dresselhaus, G., Dresselhaus, M.S., *Physical Properties of Carbon Nanotubes*. Imperial College Press, 1998.
- [14] Li, J., Cassell, A., Delzeit, L., Han, J., Meyyappan, M., 2002. Novel three-dimensional electrodes: electrochemical properties of carbon nanotube ensembles. *Journal of Physical Chemistry B* **106**(36), 9299–9305.
- [15] Azamian, B.R., Davis, J.J., Coleman, K.S., Bagshaw, C.B., Green, M.L., 2002. Bioelectrochemical single-walled carbon nanotubes. *Journal of the American Chemical Society* **124**(43), 12664–12665.
- [16] Taurino, I., Carrara, S., Giorcelli, M., Tagliaferro, A., De Micheli, G., 2011b. Comparing sensitivities of differently oriented multi-walled carbon nanotubes integrated on silicon wafer for electrochemical biosensors. *Sensors and Actuators B: Chemical* **160**(1), 327–333.
- [17] Musameh, M., Wang, J., Merkoci, A., Lin, Y., 2002. Low-potential stable NADH detection at carbon-nanotube-modified glassy carbon electrodes. *Electrochemistry Communications* **4**(10), 743–746.
- [18] Wang, J., Kawde, A-N., Musameh, M., 2003a. Carbon-nanotube-modified glassy carbon electrodes for amplified label-free electrochemical detection of DNA hybridization. *Analyst* **128**(7), 912–916.
- [19] Wu, K., Sun, Y., Hu, S., 2003. Development of an amperometric indole-3-acetic acid sensor based on carbon nanotubes film coated glassy carbon electrode. *Sensors and Actuators B: Chemical* **96**(3), 658–662.
- [20] Zhang, J., Gao, L., 2007. Dispersion of multiwall carbon nanotubes by sodium dodecyl sulfate for preparation of modified electrodes toward detecting hydrogen peroxide. *Materials Letters* **61**(17), 3571–3574.
- [21] Moore, R.R., Banks, C.E., Compton, R.G., 2004. Basal plane pyrolytic graphite modified electrodes: comparison of carbon nanotubes and graphite powder as electrocatalysts. *Analytical Chemistry* **76**(10), 2677–2682.
- [22] Wang, J., Li, M., Shi, Z., Li, N., Gu, Z., 2002. Direct electrochemistry of cytochrome c at a glassy carbon electrode modified with single-wall carbon nanotubes. *Analytical Chemistry* **74**(9), 1993–1997.
- [23] Britto, P., Santhanam, K., Ajayan, P., 1996. Carbon nanotube electrode for oxidation of dopamine. *Bioelectrochemistry and Bioenergetics* **41**(1), 121–125.
- [24] Boero, C., Carrara, S., Del Vecchio, G., Calzà, L., De Micheli, G., 2011a. Highly sensitive carbon nanotube-based sensing for lactate and glucose monitoring in cell culture. *NanoBioscience, IEEE Transactions on* **10**(1), 59–67.
- [25] Taurino, I., Carrara, S., Giorcelli, M., Tagliaferro, A., De Micheli, G., 2011a. Comparing sensitivities of differently oriented multi-walled carbon nanotubes integrated on silicon wafer for electrochemical biosensors. *Sensors and Actuators B: Chemical*. **160**(1), 327–333.
- [26] Withey, G., Lazareck, A., Tzolov, M., *et al.* 2006. Ultra-high redox enzyme signal transduction using highly ordered carbon nanotube array electrodes. *Biosensors and Bioelectronics* **21**(8), 1560–1565.
- [27] Liu, Z., Shen, Z., Zhu, T. *et al.* 2000. Organizing single-walled carbon nanotubes on gold using a wet chemical self-assembling technique. *Langmuir* **16**(8), 3569–3573.
- [28] Gooding, J.J., Wibowo, R., Liu, J., *et al.* 2003. Protein electrochemistry using aligned carbon nanotube arrays. *Journal of the American Chemical Society* **125**(30), 9006–9007.
- [29] Valentini, F., Amine, A., Orlanducci, S., Terranova, M.L., Palleschi, G., 2003. Carbon nanotube purification: preparation and characterization of carbon nanotube paste electrodes. *Analytical Chemistry* **75**(20), 5413–5421.

- [30] Wang, J., Musameh, M., 2004. Carbon nanotube screen-printed electrochemical sensors. *Analyst* **129**(1), 1–2.
- [31] Gao, M., DAL, L., Wallace, G., 2003. Glucose sensors based on glucose-oxidase-containing polypyrrole/aligned carbon nanotube coaxial nanowire electrodes. *Synthetic Metals* **137** (1–3), 1393–1394.
- [32] Dhand, C., Arya, S.K., Datta, M., Malhotra, B., 2008. Polyaniline-carbon nanotube composite film for cholesterol biosensor. *Analytical Biochemistry* **383**(2), 194–199.
- [33] Wang, J., Musameh, M., Lin, Y., 2003b. Solubilization of carbon nanotubes by Nafion toward the preparation of amperometric biosensors. *Journal of the American Chemical Society* **125**(9), 2408–2409.
- [34] Tsai, Y.-C., Li, S.-C., Chen, J.-M., 2005. Cast thin film biosensor design based on a nafion backbone, a multiwalled carbon nanotube conduit, and a glucose oxidase function. *Langmuir* **21**(8), 3653–3658.
- [35] Cavallini, A., De Micheli, G., Carrara, S., 2011. Comparison of three methods of biocompatible multi-walled carbon nanotubes confinement for the development of implantable amperometric adenosine-5-triphosphate biosensors. *Sensor Letters* **9**(5), 1838–1844.
- [36] Deng, C., Chen, J., Nie, Z., Si, S., 2010. A sensitive and stable biosensor based on the direct electrochemistry of glucose oxidase assembled layer-by-layer at the multiwall carbon nanotube-modified electrode. *Biosensors and Bioelectronics* **26**(1), 213–219.
- [37] Wang, Y., Wang, X., Wu, B. *et al.* 2008. Dispersion of single-walled carbon nanotubes in poly (diallyldimethylammonium chloride) for preparation of a glucose biosensor. *Sensors and Actuators B: Chemical* **130**(2), 809–815.
- [38] Smart, S., Cassidy, A., Lu, G., Martin, D., 2006. The biocompatibility of carbon nanotubes. *Carbon* **44**(6), 1034–1047.
- [39] Hussain, M., Kabir, M., Sood, A., 2009. On the cytotoxicity of carbon nanotubes. *Current Science* **96**(5), 664–673.
- [40] de Montellano, P.R.O., *Cytochrome P450: Structure, Mechanism, and Biochemistry*. Springer, 2004.
- [41] Werck-Reichhart, D., Feyereisen, R., 2000. Cytochromes P450: a success story. *Genome Biology* **1**(6), 3003.3001–3003.3009.
- [42] Guengerich, F.P., 2007. Cytochrome P450 and chemical toxicology. *Chemical Research in Toxicology* **21**(1), 70–83.
- [43] Guengerich, F. Human cytochrome P450 enzymes. *Cytochrome P450*, pp. 377–530. Plenum, 2005.
- [44] Johnson, D., Lewis, B., Elliot, D., Miners, J., Martin, L., 2005. Electrochemical characterisation of the human cytochrome P450 CYP2C9. *Biochemical Pharmacology* **69** (10), 1533–1541.
- [45] Bard, A.J., Faulkner, L.R., *Electrochemical Methods: Fundamentals and Applications*. Wiley, 1980.
- [46] Armstrong, F.A., Heering, H.A., Hirst, J., 1997. Reaction of complex metalloproteins studied by protein-film voltammetry. *Chemical Society Reviews* **26**(3), 169–179.
- [47] Carrara, S., Cavallini, A., Erokhin, V., De Micheli, G., 2011. Multi-panel drugs detection in human serum for personalized therapy. *Biosensors and Bioelectronics* **26**(9), 3914–3919.
- [48] Smith, A., Datta, S.P., Smith, G.H. *et al.* *Oxford Dictionary of Biochemistry and Molecular Biology*. Oxford University Press, 2000.
- [49] Asuri, P., Bale, S.S., Pangule, R.C. *et al.* 2007. Structure, function, and stability of enzymes covalently attached to single-walled carbon nanotubes. *Langmuir* **23**(24), 12318–12321.
- [50] Lyons, M.E., 2008. Carbon nanotube based modified electrode biosensors. Part 1. Electrochemical studies of the flavin group redox kinetics at SWCNT/glucose oxidase composite modified electrodes. *International Journal of Electrochemical Science* **3**, 819–853.
- [51] Juma, F., Rogers, H., Trounce, J., 2012. Pharmacokinetics of cyclophosphamide and alkylating activity in man after intravenous and oral administration. *British Journal of Clinical Pharmacology* **8**(3), 209–217.
- [52] Baj-Rossi, C., Micheli, G.D., Carrara, S., 2012. Electrochemical detection of anti-breast-cancer agents in human serum by cytochrome P450-coated carbon nanotubes. *Sensors* **12**(5), 6520–6537.
- [53] Boero, C., Carrara, S., Del Vecchio, G., Calzà, L., De Micheli, G., 2011b. Targeting of multiple metabolites in neural cells monitored by using protein-based carbon nanotubes. *Sensors and Actuators B: Chemical* **157**(1), 216–224.
- [54] Carrara, S., Shumyantseva, V.V., Archakov, A.I., Samorì, B., 2008. Screen-printed electrodes based on carbon nanotubes and cytochrome P450 for highly sensitive cholesterol biosensors. *Biosensors and Bioelectronics* **24**(1), 148–150.
- [55] Cavallini, A., Carrara, S., De Micheli, G., Erokhin, V., P450-mediated electrochemical sensing of drugs in human plasma for personalized therapy. Ph.D. Research in Microelectronics and Electronics (PRIME), 2010 Conference on, pp. 1–4. IEEE, 2010.
- [56] Gross, A.S., 2002. Best practice in therapeutic drug monitoring. *British Journal of Clinical Pharmacology* **46**(2), 95–99.
- [57] Hiemke, C., 2008. Clinical utility of drug measurement and pharmacokinetics—therapeutic drug monitoring in psychiatry. *European Journal of Clinical Pharmacology* **64**(2), 159–166.
- [58] Nicoll, D., McPhee, S.J., Pignone, M., Therapeutic drug monitoring: principles and interpretation. *Pocket Guide to Diagnostic Tests*, pp. 191–193. Lange Medical Books/McGraw-Hill, 2001.
- [59] Bonard, J.-M., Kind, H., Stöckli, T., Nilsson, L.-O., 2001. Field emission from carbon nanotubes: the first five years. *Solid-State Electronics* **45**(6), 893–914.